

<https://doi.org/10.37501/soilsa/204389>

# Potentially toxic elements and radionuclides contamination in soils from the vicinity of an ancient mercury mine in Huancavelica, Peru

Miguel Angel Castillo Corzo<sup>1\*</sup>, Víctor Antonio Peña Rodríguez<sup>1</sup>, Manuel Alberto Manrique Nugent<sup>2</sup>, Eduardo G. Villarreyes Peña<sup>1</sup>, Patrick Byrne<sup>3</sup>, Juan Carlos Gonzalez<sup>1</sup>, Galo Patiño Camargo<sup>1</sup>, Crispin H.W. Barnes<sup>4</sup>, Jesús Félix Sánchez Ortiz<sup>1</sup>, José Saldaña Tovar<sup>5</sup>, Luis De Los Santos Valladares<sup>4\*</sup>

<sup>1</sup>Facultad de Ciencias Físicas, Universidad Nacional Mayor de San Marcos, P.O Box 14-0149, Lima, Peru

<sup>2</sup>Universidad Nacional Autónoma de Huanta, Jr. Manco Cápac 497, Huanta, Ayacucho, Peru

<sup>3</sup>School of Biological and Environmental Sciences, Liverpool John Moores University, Liverpool L3 3AF, UK

<sup>4</sup>Cavendish Laboratory, Department of Physics, University of Cambridge, J.J. Thomson Ave., Cambridge CB3 0HE, UK

<sup>5</sup>Facultad de Ciencias Matemáticas, Universidad Nacional Mayor de San Marcos, P.O Box 14-0149, Lima, Peru

\* Corresponding authors: Miguel Ángel Castillo Corzo, email: [mcastilloc@unmsm.edu.pe](mailto:mcastilloc@unmsm.edu.pe), ORCID iD: <https://orcid.org/0000-0002-2652-799X>; Luis De Los Santos Valladares, email: [ld301@cam.ac.uk](mailto:ld301@cam.ac.uk), ORCID iD: <https://orcid.org/0000-0001-5930-9916>

## Abstract

Received: 2024-08-20

Accepted: 2025-04-25

Published online: 2025-04-25

Associated editor: Lukasz Uzarowicz

## Keywords:

Contaminated soils

Potentially Toxic Elements

NORM

Mercury mining

Abandoned mine

Mining activities can release large amounts of potentially toxic elements (PTE) and radionuclides in an uncontrolled manner, causing environmental contamination. This work looks at the PTE and radionuclide levels in Huancavelica, a Peruvian Andean city where the ancient mercury mine Santa Barbara operated for about five centuries, from 1573 to 1970. Although the mine closed in 1970, reports indicate that PTE contamination persists. Five representative soil samples were collected from the north, south, east and west sides of the city near the Huancavelica River. The samples were analyzed by X-ray fluorescence spectroscopy (XRF), Inductively Coupled Plasma – Mass Spectroscopy (ICP-MS) and Gamma Spectroscopy. High contamination levels of As, Cd, Pb, Zn, Ni and Cu, while low levels of Hg and Cr were found compared to the local and international standards. The highest concentration Ni (184.3 mg kg<sup>-1</sup>), Cu (1223 mg kg<sup>-1</sup>), Zn (1526 mg kg<sup>-1</sup>), Cd (11.41 mg kg<sup>-1</sup>) and Hg (6.2 mg kg<sup>-1</sup>) were found in Yananaco, the district closest to the mine. This area also showed the presence of calcite. In addition, the specific activities of the three naturally occurring radioactive materials (NORM) varied: <sup>226</sup>Ra from 38.0 to 137.3 Bq kg<sup>-1</sup>, <sup>232</sup>Th from 40.1 to 50.5 Bq kg<sup>-1</sup>, and <sup>40</sup>K from 505.5 to 793.3 Bq kg<sup>-1</sup>. The average absorbed dose rate (*D*) for the samples was 85.9 nGy/h, which is 1.7 times higher than the global average. Similarly, the average Annual Effective Dose (*E*) was 0.105 mSv/y, 1.5 times higher than the world average. Furthermore, the data reveal strong positive Pearson correlations for Hg-Ni pairs (0.981) and <sup>226</sup>Ra-<sup>232</sup>Th (0.960). Negative correlations were found for <sup>226</sup>Ra-As pairs (-0.984) and <sup>232</sup>Th-As (-0.962). These results indicate that historical mercury extraction activities increased exposure of PTE and NORM in Huancavelica. This contamination remains in areas near the abandoned mine today.

## 1. Introduction

Potentially toxic elements (PTE) are released from soils either naturally (e.g., through erosion) or anthropogenically (e.g., mining activities). Environmental and biological samples have often the highest concentration close to mines, with levels decreasing as distance increases (Puga et al., 2006; Hunter et al., 2024). In the case of mercury (Hg), its exposition occurs natural-

ly through mineral degradation, volcanic eruptions, and evaporation from land and water, among other ways (Bishop, 2020). Natural mercury mainly occurs in the form of cinnabar (HgS), originated from hydrothermal mineralisation processes associated to volcanic activity (Steinnes, 1995; Kabata et al., 2007). Whereas, the main sources of anthropogenic contamination with Hg results from mining, smelting of minerals, combustion of fossil fuels, waste incineration and the industrial production

Supplementary materials are available at: <https://www.editorialsystem.com/editor/soilsa/js/article/204389/downloadFile/10338/b952d085436c85f3ed223f389631ad5d/>

of sodium hydroxide and chloride. Trace amounts also come from fertilisers used in agriculture (Steinnes, 1995; Dev Singh et al., 2023). It is also well known that Hg does not degrade in the environment. It can move easily due to its high volatility and be transported within air masses over very long distances (Torres et al., 2022; Dev Singh et al., 2023). Its volatilization to the air occurs in the form of  $\text{Hg}^0$  (Gworek et al., 2020). Typically, the background concentration of Hg in soil ranges from 0.03 to 0.1  $\text{mg kg}^{-1}$ , with an average value of 0.06  $\text{mg kg}^{-1}$  (Gworek et al., 2020). In rural soils, total Hg concentrations vary from 0.07 to 1.22  $\text{mg kg}^{-1}$ , with a mean value of 0.13  $\text{mg kg}^{-1}$ . Urban soils show higher total concentrations, ranging from 0.07 to 1.53  $\text{mg kg}^{-1}$ , with a mean of 0.35  $\text{mg kg}^{-1}$  (Wang et al., 2012; Agency, 2007; Li et al., 2018). Soils with Hg levels 2–4 times higher than background values are considered contaminated (Agency, 2007; Wang et al., 2012; Li et al., 2018; Gworek et al., 2020). According to the Land Use and Coverage Area frame Survey (LUCAS) program from the European Commission, the average Hg concentration in over 23,000 topsoil samples (upper 20 cm) collected across Europe is 0.04  $\text{mg kg}^{-1}$ , with a range of 0 to 159  $\text{mg kg}^{-1}$  (Tóth et al., 2016). The natural/background Hg levels in other parts of the world are similar, such as 0.08  $\text{mg kg}^{-1}$  in Brazil (Lima et al., 2015), 0.05  $\text{mg kg}^{-1}$  in India (Sharma et al., 2015), 0.23  $\text{mg kg}^{-1}$  in New Zealand (Taylor, 2015), 0.11  $\text{mg kg}^{-1}$  in the Norwegian Arctic (Halbach et al., 2017) and 0.4  $\text{mg kg}^{-1}$  in Paris (Bailey et al., 2002).

The highest levels of Hg are found in soils nearby Hg mines. For example, Almaden, Spain, has a Hg concentration of 8889  $\text{mg kg}^{-1}$  from its 2000 years-old operating mine (Higuera et al., 2003). In Indrija, Slovenia, a mine that has operated for 500 years shows up to 2759  $\text{mg kg}^{-1}$  of Hg concentration (Gnamuš et al., 2000; Gosar et al., 2006). In Alaska Paris, the Hg concentration reaches 5326  $\text{mg kg}^{-1}$  (Bailey et al., 2002). In contrast, non-mining areas report much lower results. For example, soil from Changchun, China, has a median Hg concentration of 0.018  $\text{mg kg}^{-1}$ , ranging from 0.012 to 0.036  $\text{mg kg}^{-1}$  (Cheng et al., 2014). Oslo, Norway, shows a median of 0.06  $\text{mg kg}^{-1}$ , with a range of 0.01 to 2.3  $\text{mg kg}^{-1}$  (Tijhuis et al., 2002). The highest median value concentrations in non-mining areas have been reported in Palermo, Italy, with 1.85  $\text{mg kg}^{-1}$  (range: 0.004–2.61  $\text{mg kg}^{-1}$ ) (Manta et al., 2002), and Glasgow, Scotland, with 1.2  $\text{mg kg}^{-1}$  (range: 0.312–5.2  $\text{mg kg}^{-1}$ ) (Rodrigues et al., 2006).

In addition to PTE, mining activities also release natural radioactivity (Hamlat et al., 2001; Al-Saleh et al., 2008; Gazineu et al., 2008; Adukpo et al., 2010; Matisoff et al., 2011; Choudhury et al., 2022; Choudhury et al., 2022). Metallic ores contain transition metals for industry, but also naturally occurring radioactive materials (NORM). These include uranium, thorium, and their radioactive progenies like radium and radon gas (Douglas et al., 2023). NORM can be found not only in uranium mines but may also in mines for non-radioactive ores (Liu et al., 2021). For example, they are present in gold mining (Choudhury et al., 2022; Atibu et al., 2022; Moshupya et al., 2022; Mohuba et al., 2022), metal mines in the copper belt (Matisoff et al., 2011; Rollog et al., 2020), zinc mining (Parmaksiz et al., 2023), phosphate rock mining (Al-Saleh et al., 2008), potassium salt mining (Perevoshchikov et al., 2022), and coal mining (Gazineu et al., 2008; Kim et

al., 2011; Galhardi et al., 2017). There is not much information about the release of radionuclides nearby Hg mines.

The Huancavelica Region sits at 3,600 meters above sea level (m a.s.l.) in the central Andes of Peru. For about 500 years, one of the main activities there was the mining of mercury. The Santa Barbara mercury mine was found and exploited by the Spanish Crown in 1573 (Robins, 2011). From 1564 to 1810, around 17,000 metric tons of Hg vapor were released into the environment (Robins, 2011). The mine closed in 1970 and is now abandoned. Today, the main economic activity in Huancavelica is agriculture, focusing on barley, wheat, corn, peas, bean, potato, opuntia, alfalfa, among others (MIDAGRI, 2009). The region is crossed by the Ichu River from South-West to North-East, covering an area of 1383.82  $\text{km}^2$  to discharge on the Mantaro river in the Junin Region. Whereas, the capital of the region is Huancavelica City, which is crossed by the river from West to East (Ayala, 2020) (Fig. 1).

Hagan et al. (2014) evaluated the residential Hg contamination in Huancavelica City by simulated gastric fluid (GI) extractions and sequential selective extractions (SEEs) analysis of powder from adobe bricks and dirt floors. The authors surveyed four different areas in the city: Santa Ana, Ascencion, Yananaco and San Cristobal (Hagan et al., 2015). They reported total mercury concentrations in adobe bricks ranging from 8.00 to 1070  $\text{mg kg}^{-1}$  and in dirt floors from 3.06 to 926  $\text{mg kg}^{-1}$ . There were significant differences between the four neighbourhood. These values exceed the Peruvian permissible standards for agricultural and residential soils, which is 6.6  $\text{mg kg}^{-1}$  (MINAM, 2017). This means that people in Huancavelica are exposed to Hg levels higher than what is safe for humans (1 to 13 mg) (Ramirez, 2008). High level of Hg in the organism can damage the kidneys, stomach, lungs and the central nervous system (CNS) (Gaioli et al., 2012). Based on the extensive work performed on more than forty samples by Hagan et al. (2014) and Robins (2011), the present study discusses the presence of both PTE and NORM in representative soil samples from the same areas.

Potential toxic elements and radionuclides in the soil can be absorbed by local plants. Animals consume these plants, allowing toxins to enter the food chain. This can harm the health of the local population. Therefore, assessing the levels of PTE and radionuclides in the area city is crucial. This is the objective of the present work, with an additional attempt to find a relationship between potential toxic elements, radionuclide activity and past mercury mining activity.

## 2. Materials and methods

### 2.1. Sample collection and preparation

The collection sites were decided following the previous assessment reported by Hagan et al. (Hagan, 2014). Hagan et al. surveyed the soil samples collected from four neighborhoods in Huancavelica City (Hagan, 2014): Santa Ana, Ascencion, Yananaco and San Cristobal. The present work also includes the Quintanilla Pampa District. The sites of collection chosen for this research are semi-urbans areas with a recent agricultural past

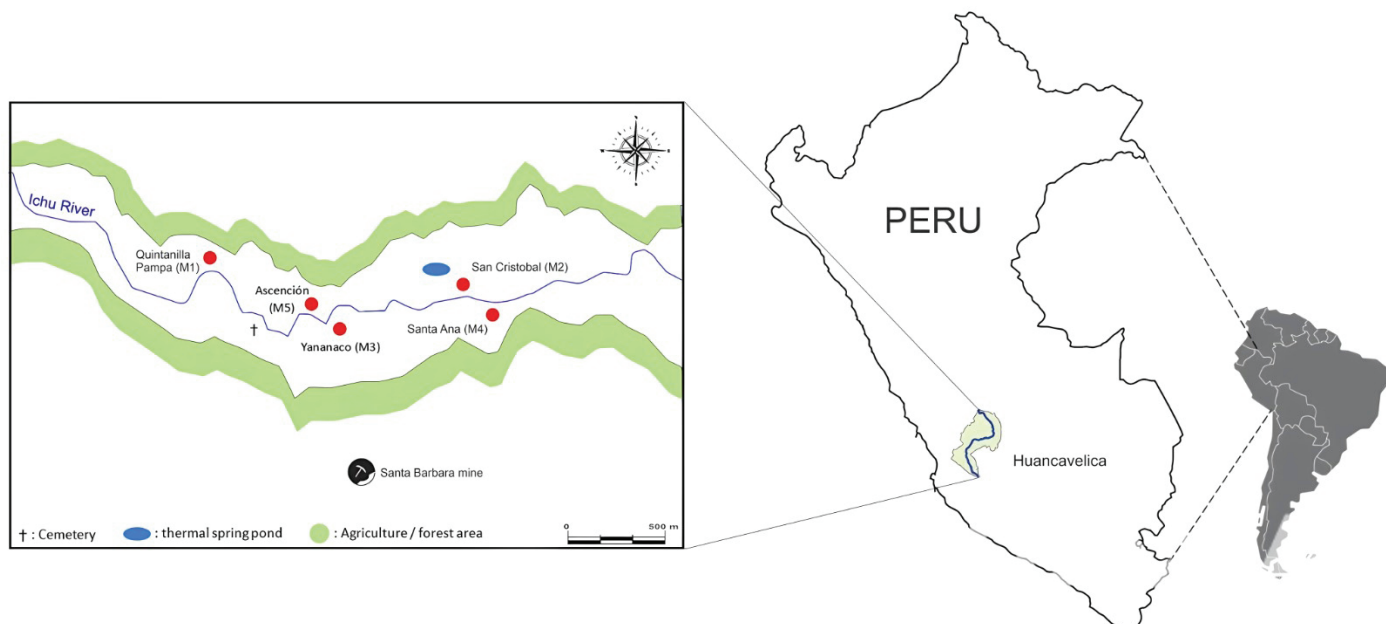


**Fig. 1.** Map of Huancavelica. The red points represent the sites of sample collection. The samples are labelled as M1 (collected from Quintanilla Pampa), M2 (collected from San Cristóbal), M3 (Yananaco), M4 (Santa Bárbara) and M5 (Ascensión)

(Fig. 1). Approximately 2 kg of soils was taken from the surface (5 cm deep) of each site (5 sites in total), placed in sterilized zip-lock bags, sealed, labelled, stored at 20°C and transported to the laboratory. Some photos taken during samples collection are presented in Fig. 1S in the Supplementary materials. The points of collection and initial details of the samples are also given in Table 1S in the Supplementary materials. Further characteristics of the samples, such as morphology and mineralogical composition are described in detail by Castillo et al. (2022). In the laboratory, the samples were dried in air to reduce humidity. For the gamma spectroscopy measurements, the samples were sieved at 200  $\mu\text{m}$  to eliminate stones, followed by drying in an oven at a temperature between 105–110°C for 24 h. The samples were then weighed, placed in Petri dishes, sealed to finally leave them between 20 to 30 days to obtain the radioactive secular equilibrium. (Baeza et al., 2003; IAEA, 2012; ISO, 2015; ISO, 2019).

## 2.2. Analytical methods

### 2.2.1. X-ray fluorescence analysis

The X-ray fluorescence (XRF) measurements were performed in a BRUKER brand total reflection X-ray Fluorescence Spectrometer, model S2-PICOFOX with a Mo tube as X-ray source. The measurement time was 2000 s. Ga was taken as the international standard for quantification and concentration of  $1 \times 10^{-3}$  kg/L. For the characterization,  $2.5 \times 10^{-5}$  kg of the pulverized powder was sieved, obtaining an approximate particle size of 44 microns. The samples were diluted in 2.50 ml of 1% triton (detergent) to achieve particles suspension. In addition, 5  $\mu\text{L}$  of  $1 \times 10^{-3}$  kg/L gallium was added as an internal standard, which allowed quantifying the elements present in the sample. The amounts mentioned above for both, triton and gallium, were appropriate calculated for the used mass ( $2.5 \times 10^{-3}$  kg). The solution

composed of these three elements was homogenized in a shaker (vortex) for 15 min at 2500 RPM. After this process, 10  $\mu\text{L}$  of the solution was pipetted onto an acrylic sample holder, which was taken to a vacuum desiccator to dry the solution. Finally, the samples were mounted in the equipment for its subsequent measurement. Considering that the measurement time per sample was 2000 s, three measurements were made for each sample.

### 2.2.2. Inductively Coupled Plasma – Mass Spectroscopy measurements

The soil samples were also analyzed by Inductively Coupled Plasma – Mass Spectroscopy (ICP-MS) (Li, Be, Na, Mg, Ca, V, Cr, Mn, Ni, Cu, Zn, Ga, As, Se, Rb, Sr, Ag, Cd, In, Cs, Ba, Tl, Pb, Bi and U) and Inductively Coupled Plasma Optical Emission Spectroscopy (ICP-OES) (Al, K, Fe, P and Si) following a reverse aqua regia digestion (EPA Method 3051A) in a microwave digestion system. A certified reference material (CRM-016) was used to assess the recovery of analytes in the sediment samples which was satisfactory (78% to 130%) for most analytes apart from Al (464%), K (276%), Ca (9%), V (186%) and Cr (183%), which were unsatisfactory.

### 2.2.3. Atomic absorption spectroscopy analysis

For the determination of the Hg component, the samples were measured in a SHIMADZU AA-7000 atomic absorption spectrometry equipment. The samples were mechanically homogenized, then 3 g of each sample were loaded in crucibles and placed in a muffle oven to be calcined. The temperature slowly increased to 150°C and then at intervals of 150°C up to 550°C, until obtaining white ashes. Once the calcination was finished, they were cooled and subjected to an acid digestion with 5 ml of  $\text{HNO}_3$  (CC) (1:1) in a thermal plate at 700°C (moderate heating to avoid total evaporation of the acid). The crucible containing

the sample was constantly shaken to eliminate the nitrous vapors until they dry. Then, the samples were cooled and distilled water was added to dissolve the contents of the glass. To prepare a  $1 \times 10^{-4}$  kg/L Hg standard, 10 mL of the  $1 \times 10^{-3}$  kg/L certified standard was poured in a 100 mL phial, measured and then quenched with ultrapure water. The lifetime of the standard is 6 months. Similar procedures were followed to obtain the calibration standards  $1 \times 10^{-8}$  kg/ $\mu$ L,  $2 \times 10^{-8}$  kg/L, and  $4 \times 10^{-8}$  kg/L.

#### 2.2.4. Gamma spectroscopy analysis

The radioactivity was measured by gamma spectroscopy, using a scintillation detector of sodium iodide doped with thallium NaI(Tl), with a  $3'' \times 3''$  crystal size, Canberra model: 802-4. The detector was connected to a Spectech brand multichannel amplifier (1024 channels) and enclosed in a 50 mm thick lead shield case to minimize background radiation. For calibration of the energy and efficiencies, reference materials from the International Atomic Energy Agency (IAEA) were used (IAEA-412, IAEA-447, RGK-1, RGU-1 and RGTh-1). Some corrections for self-absorption and random addition were also made for the calculation of the activity. All the samples were sealed in Petri dishes of approximately 100–95 g volume and left under normal conditions of pressure and temperature for 30 days. This allows the uranium-238 family and the intermediate daughters (such as radium-226 and radon-222) to reach the secular equilibrium, and thus to obtain representative activity values for the father uranium by the detector for 86400 s (Quintana et al., 2004; International Agency Atomic Energy, 2011; International Agency Atomic Energy, 2016; International Agency Atomic Energy, 2016; International Agency Atomic Energy, 2019; International Agency Atomic Energy, 2021).

For the identification of the most natural occurring radioactive materials (NORM)  $^{226}\text{Ra}$ ,  $^{40}\text{K}$  and  $^{232}\text{Th}$ , the following photopeaks: 351.9 keV corresponding to  $^{214}\text{Pb}$ ; 1460.8 keV corresponding to  $^{40}\text{K}$ , and 2614.5 keV corresponding to  $^{208}\text{Tl}$  were analyzed (ISO:18589-3, 2015). In the present work, any presence of technologically enhanced naturally occurring radioactive materials (TENORM) has been considered. For the determination of the activity per unit of mass ( $A$ ) of K-40, Ra-226 and Th-232 for the soil samples, the following relation was applied:

$$A = \frac{N_n}{I \varepsilon m t_r f_c} \quad (1)$$

where  $N_n$  is net counts of the photo-peak,  $I$  is the probability for the gamma transition,  $\varepsilon$  is the efficiency of the detector for the determination of the photo-peak,  $m$  is the mass of the sample,  $t_r$  is the time counting for the samples and  $f_c$  is the correction factor where after calibration a value of 0.981 was determined, where self-absorption, decay, random sum and sum by coincidences were considered. (ISO:18589-3, 2015; ISO: 19581, 2019). The specific activities in  $\text{Bq kg}^{-1}$  of the main naturally occurring radioactive materials (NORM), such as  $^{40}\text{K}$ ,  $^{226}\text{Ra}$ , and  $^{232}\text{Th}$ , in the soil samples were also obtained by gamma spectroscopy. By analyzing the spectra, the distribution of NORM across the sites of samples collection was studied. The photopeaks were analyzed using Equation (1) providing precise quantification of these radionuclides in the samples.

The measurement of the radiological risk linked to radionuclides exposure in the ground (up to 1 m), is carried out using the Absorbed Dose Rate ( $D$ ) or the gamma dose rate in the air. In this way, the following equation relates the activities between  $^{226}\text{Ra}$ ,  $^{232}\text{Th}$  and  $^{40}\text{K}$  in  $\text{Bq kg}^{-1}$ .

$$D(\text{nGy/h}) = 0.462 A_{\text{Ra}} + 0.604 A_{\text{Th}} + 0.0417 \quad (2)$$

The Annual Effective Dose ( $E$ ) is a parameter used in radiation protection that quantifies the radiation absorbed by a person per year. Its application is common in research on environmental radiation, allowing the potential risk of exposure to be evaluated and establishing the safe dose limits. In the present work, it is determined by the following equation.

$$E(\text{mSv/y}) = D \times 8760 \times 0.2 \times 0.7 \times 10^{-6} \quad (3)$$

where  $D$  represents the absorbed dose rate. The annual time is 8760 h; while 0.7 ( $\text{mSv/y}$ ) and 0.2 are the conversion factors for converting the absorbed dose in the air into the effective dose in air, and the proposed occupational factor, respectively (Baeza et al., 2003).

Radium equivalent activity ( $Ra_{\text{eq}}$ ) is a term used to describe the content of  $^{226}\text{Ra}$ ,  $^{232}\text{Th}$  and  $^{40}\text{K}$  in a radioactive substance (in  $\text{Bq kg}^{-1}$ ). This concept is based on the idea that radiation from radium, thorium and potassium can have a biological effect, similar to that of a specific amount of the radium and radon descendants. Its calculation is carried out using the following equation:

$$Ra_{\text{eq}}(\text{Bq kg}^{-1}) = A_{\text{Ra}} + 1.43 A_{\text{Th}} + 0.077 A_{\text{K}} \quad (4)$$

where  $A_{\text{Ra}}$  is the activity of  $^{226}\text{Ra}$ ,  $A_{\text{Th}}$  is the activity of  $^{232}\text{Th}$  and  $A_{\text{K}}$  is the activity of  $^{40}\text{K}$ .

### 3. Results and discussion

The soil samples contain grains with different colour, shape and sizes as discussed in our previous work (Castillo et al., 2022). These differences depend on the chemical composition of the grains (De Los Santos et al., 2024). The present work focuses on the PTE and radionuclides present in the samples. Other components, like transition metals, are detailed in the Supplementary materials (Section 1S). The main elements in the soil samples include Si, Ca, Al, K, Fe and Ti, as expected since the main composition of soils are quartz ( $\text{SiO}_2$ ) and aluminium silicates (De Los Santos et al., 2022). The next sections will cover the PTE and radionuclides in the samples and how their amount may have been enhanced by the mercury mining activities in the past.

#### 3.1. Potentially toxic elements

In addition to the transition metals, Table 2S in the supplementary materials also reveals the presence of the potential toxic elements: arsenic (As), lead (Pb), and cadmium (Cd) in the samples. However, the concentration data obtained by XRF rep-

resents localized information on the concentration in selected areas of the samples surface. The total concentration of the PTE in the samples was obtained by ICP-MS technique and are listed in Table 1. The differences between the information obtained by XRF (shown in Table 2S) and those obtained by ICP-MS are explained in further detail elsewhere (De Los Santos et al., 2024).

Arsenic was detected on the surface of all five samples using XRF. According to Table 2S (see Supplementary materials), sample M2 has the highest amount of arsenic, measuring  $0.38(2) \times 10^{-3} \text{ mg kg}^{-1}$ , while sample M4 contains the lowest amount, at  $0.06(1) \times 10^{-3} \text{ mg kg}^{-1}$ . These results are consistent with the measurements obtained by ICP-MS, which show the highest total As concentration in samples M2 ( $815.7 \text{ mg kg}^{-1}$ ) and the lowest in sample M4 ( $33.4 \text{ mg kg}^{-1}$ ), as noted in Table 1. Arsenic does not exist as a pure element; it tends to bond chemically with many other elements (Nazari et al., 2017). It is derived from natural enargite ( $\text{Cu}_3\text{AsS}_4$ ) which can be found in certain soils, rocks and river sediments throughout the Peruvian Andes (De Los Santos et al., 2022) and is distributed through fluvial and aeolian transport processes (Schnitzer et al., 1964). The permissible level of arsenic in agricultural and residential soils in Peru is  $50 \text{ mg kg}^{-1}$ , as indicated in Tables 1 and 3S, as well as in the reference (MINAM, 2017). This suggests that, except for Sample M4, soils in Huancavelica City are contaminated with As. The high levels of As found in this study indicate that the *San Cristóbal* neighborhood is the most polluted area concerning arsenic contamination. Thus, in addition to the natural As, present in the Andean mountains (Bech et al., 1997; Tapia et al., 2019), the high levels reported in the present work should have been caused during mercury extraction, as it is well-known that it is enhanced by mining activities (Williams et al., 1996; Bissen et al., 2003; Satoshi et al., 2003; Paktun et al., 2004; Cancès et al., 2008).

The ICP-MS analysis reveals that the levels of Pb in most sites exceed  $140 \text{ mg kg}^{-1}$ , which is the maximum permissible limit for urban areas (see Tables 1 and 3S). The only exception is site M4, where the Pb level is approximately  $20 \text{ mg kg}^{-1}$ . According to the data, lead contamination in the area is distributed as follows:  $M2 > M5 > M3 > M1 > M4$ , with sample M2 showing the highest level at approximately  $1700 \text{ mg kg}^{-1}$ . Lead contamina-

tion around the world comes from gasoline, welding used in water pipes, ammunition, and lead-based paints (Bergdahl, 2022). However, this does not seem to apply in Huancavelica, where houses are typically constructed with plumbing made of plastic, there is minimal use of paints, and the number of cars per thousand inhabitants is only 3 (MTC, 2022). Therefore, other natural or anthropogenic sources of lead should be considered. If the source is natural, the high Pb concentrations may originate from cerussite, a lead (II) carbonate ( $\text{PbCO}_3$ ) that is insoluble in water. The solubility product is approximately  $[\text{Pb}^{2+}][\text{CO}_3^{2-}] \approx 1.5 \times 10^{-13}$  at  $25^\circ\text{C}$ , as discussed in section 4S of the Supplemental material.

If the Pb contamination in Huancavelica is anthropogenic, it could originate from various sources (Ponce et al., 2024). One possible source is the past smelting of ores, as Pb has a low melting point (approximately  $327^\circ\text{C}$ ) and is easily released into the environment. However, the highest level of Pb are found in the northeastern part of Huancavelica City, particularly in San Cristóbal neighborhood (Site M2), crossing the Ichu River and away from the abandoned mine. This suggests that Pb might have been transported by rainfall and erosion. Similar situations have been reported in other parts of the world (Foulds et al., 2014). Other potential source of lead contamination could be related to agricultural activities. For example, elevated Pb concentrations ( $> 1200 \text{ mg kg}^{-1}$ ) have been detected in cultivated fields nearby a similar mine in Huaral, located on the coast of Peru (Van Geen et al., 2012). In that case, the high levels of lead may have originated from lead arsenate ( $\text{Pb}_3(\text{AsO}_4)_2$ ), which local farmers extensively used as an insecticide against pests affecting potatoes until a decade ago. This insecticide is highly persistent, and its use was banned by the Peruvian Ministry of the Environment at the end 2013 (SENASA, 2012).

The average concentration of Pb in the blood of healthy, unexposed adults is estimated at  $0.9 \mu\text{g/dL}$  (Bakr et al., 2023). The reference values for permissible blood Pb levels are less than  $5 \mu\text{g/dL}$  in adults and less than  $3.5 \mu\text{g/dL}$  in children. In contrast, critical or hazardous levels are defined as  $70 \mu\text{g/dL}$  and above in adults, and  $20 \mu\text{g/dL}$  in children (CDC, 2022). Alarmingly, over 80% of children living near mining areas in Peru have been found to have blood levels higher than  $10 \mu\text{g/dL}$  (Van Geen et al.,

**Table 1**

Contents of trace elements (in  $\text{mg kg}^{-1}$ ) in soils collected from Huancavelica and environmental quality standards for classifying agricultural, urban and industrial soils from Peru (in  $\text{mg kg}^{-1}$ )

Sample	Cr	Ni	Cu	Zn	As	Cd	Pb	Hg
M1	80.7	137.6	301.7	955.0	706.5	1.5	186.6	4.5
M2	28.1	31.0	44.5	1344	815.7	6.0	1699	2.7
M3	57.2	184.3	1223	1526	480.8	11.4	140.5	6.2
M4	30.0	20.2	20.02	114.3	33.4	Bdl	20.3	1.7
M5	51.3	90.6	454.6	622.4	638.4	1.3	304.9	3.8
Agricultural soil	NI	NI	NI	NI	50	1.4	70	6.6
Urban soil	400	NI	NI	NI	50	10	140	6.6
Industrial soil	1000	NI	NI	NI	140	22	800	24

Explanations: Bdl= Below detection limit; NI: There is no information.

2012; Castro et al., 2013), which may also be the case in Huancavelica. Lead is toxic because it can mimic calcium in the body, as the ions  $Pb^{2+}$  and  $Ca^{2+}$  are of similar size. Consequently, lead can replace calcium in various critical processes that depend on this mineral.

As indicated in Table 2S, Hg was detected on the soil surface from Yananaco ( $\sim 143.6 \pm 14.4$ )  $mg\ kg^{-1}$  and Asención ( $21.37 \pm 2.24$ )  $mg\ kg^{-1}$  districts. According to the ICP-MS data presented in Table 1, sample M3 (Yananaco) contains the greatest concentration of total mercury ( $\sim 6.2$ )  $mg\ Kg^{-1}$ , whereas sample M4 (Santa Ana) has the lowest amount ( $\sim 1.7$ )  $mg\ kg^{-1}$ . These results are consistent to those obtained by Robins et al. (2011) and Hagan et al. (2014, 2015), indicating that the concentration of Hg is highest near the mine, and diminishes with distance (see Table 5S). Metallic mercury is rarely found in natural conditions; instead, it typically forms complexes in soil minerals because of its absorption by either inorganic mineral surfaces or organic matter. Mercuric cation  $Hg^{2+}$  (Hg(II)) has a strong tendency to form covalent bonds with  $Cl^-$ ,  $OH^-$ , and  $S^{2-}$  anions which are usually present in the humic matter presents in soils (Steinnes, 1995; Agency for Toxic Substances and Disease Registry, 1999; Steinnes et al., 2003). Thus,  $Hg^{2+}$  with electronical valence configuration  $6s^2$  is the most frequent mercury ion. Besides,  $Hg^0$  is not detected in soils (Biester et al., 2002; Gilli et al., 2018; Osterwalder et al., 2019). However, it precipitates as  $Hg^{2+}S^{2-}$  (mercuric sulphide, cinnabar, red in colour) at increased redox potential. This is the most significant natural source of mercury and is insoluble in water. Nevertheless,  $Hg^0$  can also be formed by microbial transformation (reduction) from Hg(II) and, due to its high volatility, it is one of the main components in the cycling of mercury between soil and air activity (Steinnes, 1995; Schlüter, 1993). Moreover, it has been reported that the volatilisation of mercury increases with increasing soil moisture content (Kabata et al., 2001), which is also the case for the agricultural soils in Huancavelica. Therefore, the fact that the total Hg levels listed in Table 1 do not exceed the permissible Peruvian norm ( $\sim 6.6$ )  $mg/kg$  (MINAM, 2017) confirms its high mobility/volatility. Further discussion of Hg in soils is provided in the Supplementary material 5S.

The results presented in this work also agree with those reported by Hagan et al., (2014) in which Santa Ana District (M4) presents the lowest level of mercury. According to Hagan *et al.*, (2014), the smelting plants of the mine were located in San Cristóbal, Yananaco and Asención Districts, but not in Santa Ana. This should be the reason why the level of mercury in sample M4 is the lowest ( $1.7$ )  $mg\ Kg^{-1}$ , in contrast to the other sites.

Geogenic Cd is more commonly abundant in sedimentary rocks than in igneous or metamorphic rocks (He et al., 2015; Kubier et al., 2019). Cadmium in soils can be present as hydroxide  $Cd(OH)_2$  and carbonate ( $CdCO_3$ ), specially at elevated pH ( $>11$ ). The standard level of cadmium in Peru for agricultural and urban soils are 1.4 and 10  $mg.kg^{-1}$ , respectively (see Table 1). The values of Cd obtained by ICP-MS were expected since the sample collection sites are urban. However, the area nearby the abandoned mine (Yananaco, M3) presents the highest level of Cd ( $11.4$ )  $mg\ kg^{-1}$ , resulted from the past mineral exploitation. As for zinc, up to date, there is no information about permissible levels in

the Peruvian regulations. Thus, the values presented in Table 1 are compared to the worldwide standards (200–400  $mg\ Kg^{-1}$ , see Table 4S in the Supplementary materials) and other works performed in other southern areas in Peru. Those work report average Zn values of 30 and 59.5  $mg\ kg^{-1}$  with maximum concentrations of 40 and 67.1  $mg\ kg^{-1}$  for the Arequipa City and the Suches River (Puno), respectively (Salas et al., 2022; Huerta et al., 2023). In contrast, the Zn concentration for all the collecting sites in the present work are very much higher (see Table 1); and similar to the case of Cd, the highest level of zinc is found in site 3 which is nearby the abandoned mine. These values reveal that Huancavelica is contaminated with Zn.

Both, cadmium and zinc are +2 ions, locate in the same subgroup of the periodic table and are usually found together in areas with industrial activities (Krishna, 2007). The fact that in the present work high concentration levels are found nearby the abandoned mine, suggests that both elements were released to the environment during the mining activity. Cadmium entering water bodies can combine with inorganic or organic ligands to form various soluble complexes, such as  $Cd(OH)^+$ ,  $Cd(OH)_2$ ,  $HCdO_2^-$  and  $CdO_2^{2-}$ , and the solubility of cadmium in natural water is mainly controlled by the concentration of a carbonate or hydroxyl groups present in the soils (Gussone et al., 2005). Mines produce toxic cadmium oxide (CdO) during the refinement of lead and zinc (Ramírez, 1986) and thus, it might be one of the origins of Cd in the present work. However, cadmium can also form precipitates with S, P, As, Cr, and other anions, although the solubility of these compounds varies depending on the pH and other chemical factors (Rahim et al., 2022).

It is well-known that Cd easily accumulates in some plants reaching higher concentration than in the soil (Florida, 2021), as might happen with the barley, wheat, corn, peas, bean, potato, opuntia and alfalfa grown in Huancavelica. After crops absorb Cd, it enters the food chain, progressively accumulating in humans, impairing kidney function, affecting the liver, and causing bone demineralization. The average range in blood level of healthy, unexposed-Cd adults is 0.1–4  $\mu g/L$  (NIOSH, 2022) and despite there are no available reports about the intake levels of Cd in the population of Huancavelica, a recent study in Andean camelids (alpacas) in the area reports a mean concentration of  $0.335 \pm 0.088$ )  $mg\ kg^{-1}$  of Cd in their muscles which exceeds the maximum level allowed by the FAO (0.2  $mg\ kg^{-1}$ ) and the European Commission (0.05  $mg\ kg^{-1}$ ) (Orellana et al., 2021). Further discussion on Cd and Zn is provided in section 6S of the supplemental material.

The permissible Cu levels in soils around the world are c.a. 50–150  $mg\ kg^{-1}$  (see Table 3S) and there is no corresponding information for the case of Peru up to date. However, in the present work, Tables 1 and 2S reveal the presence of copper in all the samples. This was expected since Cu is common in some regions of Peru (De los Santos, et al., 2022).

Similar to the case of Cu, there is no information about standard levels of Ni in Peru. However, the available information for other countries states c.a. 50–100  $mg\ kg^{-1}$  (see Table 1). In the present work, the lowest level of Ni is found in sample M4 (20.2  $mg\ kg^{-1}$ ), while the highest level is found in Sample 3 (184.3  $mg\ kg^{-1}$ ). These levels are very high when compared to those found

in other areas of Peru. For example, Fernández et al. (2022) found that the medium and maximum levels of Ni in Tiquillaca, Puno (Southeastern Peru) are 1.72 and 3 mg kg<sup>-1</sup>, respectively. These findings reveal that Huancavelica is also polluted with Ni. Furthermore, it suggests that the historical mining activities enhanced the exposition of different potential toxic elements in the area. In this regard, it has been well documented that Ni compounds, such as nickel subsulfide (Ni<sub>3</sub>S<sub>2</sub>), nickel oxide and nickel carbonyl induce acute pneumonitis, central nervous system disorders, skin disorders (such as dermatitis), and cancer of the lungs and nasal cavity (Waldron, 1980; Smialowicz et al., 1984; Benson et al., 1995). As an example from other cases around the world, pregnant female workers at a Russian nickel hydrometallurgy refining plant showed a marked increase in frequency of spontaneous and threatening abortions and in structural malformations of the heart and musculoskeletal system in their born babies (Chashschin et al., 1994).

According to Table 1, the permissible level by the Environmental Ministry of Peru for Cr in urban and industrial soils are 400 and 1000 mg kg<sup>-1</sup>, respectively. There is no information for the case of agricultural soils. However, the corresponding level in other countries lies between 100 to 200 mg kg<sup>-1</sup> (see Table 4S in the Supplementary materials). The levels of chromium found for the soil collected in the present work are lower than 100 mg kg<sup>-1</sup> (the lowest concentration is 28.1 mg kg<sup>-1</sup> for Sample 2 and the highest one is 80.7 mg kg<sup>-1</sup> for Sample 1). These values reveal that Huancavelica city is not contaminated with chromium.

### 3.2. Radionuclides

The gamma spectra for all the samples are shown in Fig. 2. They have been inspected in three energy ranges located at 351.92 keV (corresponding to <sup>214</sup>Pb, a decay product of <sup>226</sup>Ra), 1460.81 keV (corresponding to <sup>40</sup>K) and 2614.50 keV (corresponding to <sup>208</sup>Tl, a decay product of <sup>232</sup>Th). Figure 2 reveals different intensities and shape of the gamma spectra among the different soil samples. This is caused by the differences in the composition and concentration of the radionuclides in the samples. However, the intensities of the photo-peaks for <sup>40</sup>K, <sup>226</sup>Ra, and <sup>232</sup>Th in the present samples are consistent with those found in other regions with similar geological activity (Handbook of Radiatioativity, 2020). The samples from Quintanilla Pampa (M1), Yananaco (M3), and Asención (M5) exhibit higher <sup>226</sup>Ra peak intensities than the other samples. This observation is confirmed with the data presented in Table 2, which indicates that these samples present high <sup>226</sup>Ra activity. In contrast, the samples from San Cristóbal (M2) and Santa Ana (M4) show moderate intensities in the <sup>226</sup>Ra peaks, reflecting a medium activity for this radionuclide (see Table 3).

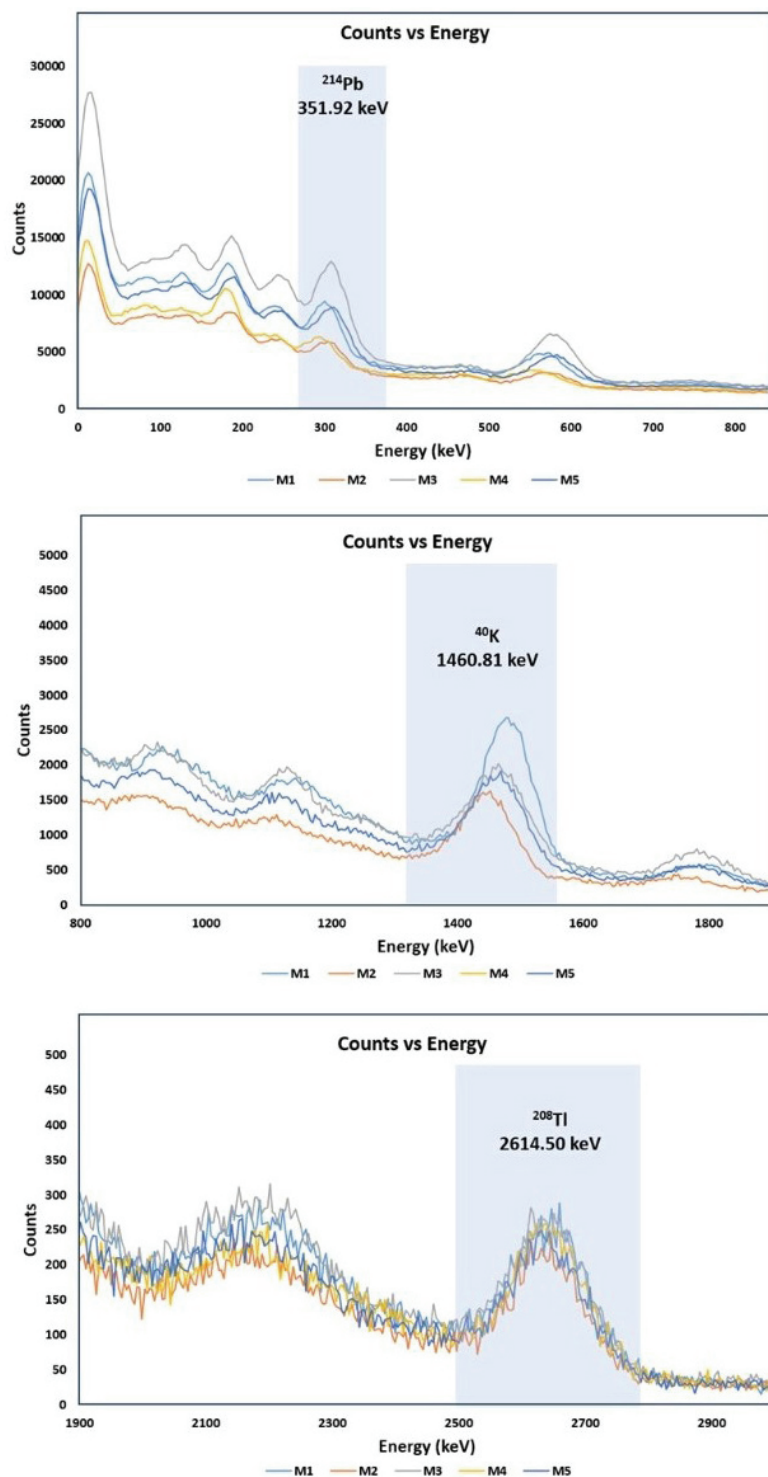


Fig. 2. Gamma spectra of the samples M1, M2, M3, M4 y M5 where the photo-peaks can be identified. a) Photo-peak at 351.92 keV for the identification of Pb-214 descendent of <sup>226</sup>Ra. b) Photo-peak at 1460.81 keV for the identification of <sup>40</sup>K. c) Photo-peak at 2614.50 keV for the identification of Tl-208 descendent of <sup>232</sup>Th, Where no significant variation is seen in the samples

Considering specific activities, the present samples are divided into two groups: those with high <sup>226</sup>Ra activity (Quintanilla Pampa (M1), Yananaco (M3), and Asención (M5)), and those with medium activity (San Cristóbal (M2) and Santa Ana (M4)), with the values listed in Tables 2 and 3. The first group shows an average <sup>226</sup>Ra activity of 97.2 Bq kg<sup>-1</sup>, which is 2.8

**Table 2**

Activities of soils samples collected from Huancavelica, Peru

SAMPLES	<sup>40</sup> K (Bq kg <sup>-1</sup> )	ΔA (Bq kg <sup>-1</sup> )	<sup>226</sup> Ra (Bq kg <sup>-1</sup> )	ΔA (Bq kg <sup>-1</sup> )	<sup>232</sup> Th (Bq kg <sup>-1</sup> )	ΔA (Bq kg <sup>-1</sup> )
M1	792.3	11.1	66.9	4.2	40.1	1.4
M3	534.3	11.1	137.3	7.1	44.8	1.6
M5	544.4	9.4	87.5	2.5	39.5	1.5
MEAN	624.0	10.5	97.2	4.6	41.5	1.5

Explanations: Activities of the soil samples M1, M3 y M5 for the NORM <sup>40</sup>K, <sup>226</sup>Ra and <sup>232</sup>Th. Where ΔA is the uncertainty of the activity. Note the high values compared to the worldwide range given by UNSCEAR-2008. (UNSCEAR, United Nations Scientific Committee on the Effects of Atomic Radiation, 2008).

**Table 3**

Average activity of soils collected from Huancavelica, Peru

Samples	<sup>40</sup> K (Bq kg <sup>-1</sup> )	ΔA (Bq kg <sup>-1</sup> )	<sup>226</sup> Ra (Bq kg <sup>-1</sup> )	ΔA (Bq kg <sup>-1</sup> )	<sup>232</sup> Th (Bq kg <sup>-1</sup> )	ΔA (Bq kg <sup>-1</sup> )
M1	505.5	10.9	51.9	2.3	40.1	1.4
M2	576.5	9.4	38.0	2.5	50.1	1.5
MEAN	541	10.15	44.95	2.4	45.3	1.45

Explanations: Average activity of the soil samples M1 and M2 for NORM <sup>40</sup>K, <sup>226</sup>Ra and <sup>232</sup>Th. Note the values lie on the worldwide range given by UNSCEAR-2008, except <sup>232</sup>Th.

times higher than the global average (35.0 Bq kg<sup>-1</sup>) and exceeds the global range (17–60 Bq kg<sup>-1</sup>). These results are similar to those previously reported by Rani et al. (2005) for regions with similar soils. The authors highlight the influence of geological characteristics on the soil's radioactive activity (Rani et al., 2005). Similarly, El-Taher A et al. (2010) reports <sup>226</sup>Ra activities significantly higher than the global average in soils from agricultural areas in Upper Egypt due to phosphorus accumulation (El-Taher et al., 2010). Furthermore, Al-Jundi et al. found that <sup>226</sup>Ra concentrations are high because the soils are close to a phosphate mine (Al-Jundi et al., 2003).

About the <sup>40</sup>K and <sup>232</sup>Th photopeaks, they also show variations among the samples. For the <sup>232</sup>Th peak, the samples yield an average of 41.5 Bq kg<sup>-1</sup>, which is 1.4 times higher than the global average (30.0 Bq kg<sup>-1</sup>), but within the global range (11–64 Bq kg<sup>-1</sup>). These <sup>232</sup>Th values are similar to those reported by Karahan et al. for soils from urban areas in Turkey, reflecting regional geological variability (Karahan et al., 2000). Eventually, for <sup>40</sup>K, the samples yielded an average of 624.0 Bq kg<sup>-1</sup>, which is 1.6 times higher than the global average (400 Bq kg<sup>-1</sup>) but within the global range (140–850 Bq kg<sup>-1</sup>). Similar to other studies, the <sup>40</sup>K peak presents a broad energy distribution due to its high presence in common soil minerals such as igneous rocks, feldspars, and natural micas. This is consistent with the findings of Lu Xinwei et al. (2012), where high <sup>40</sup>K values in soils were reported (Xinwei et al., 2006). There are also similarities with the findings of Beretka and Mathew (1985), who reported high <sup>40</sup>K values in soils derived from igneous rocks (Beretka et al., 1985).

For M2 and M4, the <sup>226</sup>Ra activity showed an average of 45 Bq kg<sup>-1</sup>, which is 1.3 times higher than the global average (35 Bq kg<sup>-1</sup>) and within the global range (17–60 Bq kg<sup>-1</sup>). The <sup>232</sup>Th activities in these samples have an average activity of 45.3 Bq kg<sup>-1</sup>, which is 1.5 times higher than the global average (30 Bq kg<sup>-1</sup>), but within the global range (11–64 Bq kg<sup>-1</sup>). This value is slightly higher than the average for the samples from the first group, indicating greater variability in the distribution of <sup>232</sup>Th in these areas of study. The <sup>40</sup>K activity in this group shows an average of 541.0 Bq kg<sup>-1</sup>, which is 1.4 times higher than the global average (400 Bq kg<sup>-1</sup>), also within the global range of (140–850 Bq kg<sup>-1</sup>) (UNSCEAR, 2008; Tsolova et al., 2022; Uzarowicz et al., 2024).

The Table 4 reveals that the absorbed dose rate (*D*), analyzed using Equation (2), resulting for the samples ranges from 69.3 nGy/h (M2) to 112.8 nGy/h (M3); with an average value of 85.9 nGy/h. The global average for outdoor terrestrial radiation is approximately 60 nGy/h (UNSCEAR, 2000). Therefore, the mean value in these samples is significantly higher, suggesting elevated background radiation levels compared to global averages. These high dose rates align with those found in areas with high natural radioactivity, such as in Kenya, in which Kaniu M.I et al. reported dose rates ranging between 60 and 965 nGy/h (Kaniu et al., 2018). Likewise, the present data are related to the highest dose found in the world by Vasconcelos (2011) in Guarapari beach, Brazil (Vasconcelos et al., 2011).

**Table 4**  
Natural radioactivity of soil samples from Huancavelica, Peru

SAMPLES	<i>D</i> (nGy/h)	<i>E</i> (mSv/y)	$R_{\text{aeq}}$ (Bq.Kg <sup>-1</sup> )
M1	88.2	0.108	185.3
M2	69.3	0.085	148.2
M3	112.8	0.138	242.5
M4	72.1	0.088	154.6
M5	87.0	0.107	185.9
MEAN	85.9	0.105	183.3

Explanations: Natural radioactivity in absorbed dose rate (*D*), effective annual equivalent dose (*E*) and equivalent activity in radio ( $R_{\text{aeq}}$ ) for soils samples collected from Huancavelica City, Peru.

The Annual Effective Dose, analyzed using Equation (3), results in values ranging from 0.085 mSv/y (M2) to 0.138 mSv/y (M3); with an average value of 0.105 mSv/y. UNSCEAR 2000 reports a global average of 0.07 mSv/y for outdoor exposure due to natural sources. The higher values in the soil samples suggest a greater annual exposure, comparable to studies in Turkey, where high natural radioactivity in soil resulted in annual effective doses up to 0.2 mSv/y (Karahan et al., 2000).

Radium equivalent activity, analyzed using Equation (4), results in values ranging from 148.2 Bq kg<sup>-1</sup> (M2) to 242.5 Bq kg<sup>-1</sup> (M3); with an average value of 183.3 Bq kg<sup>-1</sup>. The UNSCEAR 2000 recommends that the safety limit for  $R_{\text{aeq}}$  is 370 Bq kg<sup>-1</sup>, which ensures that the radiation dose does not exceed 1 mSv/y. The values for all samples are well below this limit, indicating that, despite higher absorbed dose rates and annual effective doses, the soil does not pose a significant radiological hazard based on  $R_{\text{aeq}}$ . This finding is consistent with studies reported

in Egypt, where soils from agricultural regions showed  $R_{\text{aeq}}$  values ranging from 200 to 300 Bq kg<sup>-1</sup> are still below the safety threshold (El-Taher et al., 2010).

### 3.3. Multivariate statistical results

In order to examine possible connections between the presence of PTE and NORM, a Pearson correlation analysis was carried out. The considered variables include the activity of <sup>226</sup>Ra, <sup>232</sup>Th and <sup>40</sup>K along with the concentrations of Cr, Ni, Cu, Zn, As, Cd, Pb and Hg for all the samples. From the obtained data (see Table 6), it is observed that there are positive correlations ( $P < 0.05$ ) for the pairs of metals Cu-Ni (0.888) and Cu-Hg (0.917). There is also positive correlations ( $P < 0.01$ ) for the Hg-Ni pairs (0.981), <sup>226</sup>Ra-<sup>232</sup>Th (0.960) and negative correlations ( $P < 0.01$ ) for <sup>226</sup>Ra-As pairs (-0.984) and <sup>232</sup>Th-As (-0.962).

**Table 5**  
Pearson correlation in elements contained in soils from Huancavelica, Peru

	Cr	Ni	Cu	Zn	As	Cd	Pb	Hg	<sup>226</sup> Ra	<sup>40</sup> K	<sup>232</sup> Th
Cr	1	0.800	0.433	0.240	0.335	-0.289	-0.487	0.702	-0.442	0.787	-0.410
Ni	0.800	1	0.880*	0.568	0.253	0.397	-0.443	0.981**	-0.407	0.318	-0.246
Cu	0.433	0.880*	1	0.571	0.058	0.695	-0.381	0.917*	-0.219	-0.146	-0.026
Zn	0.240	0.568	0.571	1	0.672	0.909	0.460	0.692	-0.714	-0.145	-0.491
As	0.335	0.253	0.058	0.672	1	-0.537	0.616	0.349	-0.984**	0.114	-0.962**
Cd	-0.289	0.397	0.695	0.909	-0.537	1	0.065	0.559	0.669	-0.516	0.912
Pb	-0.487	-0.443	-0.381	0.460	0.616	0.065	1	-0.292	-0.494	-0.402	-0.469
Hg	0.702	0.981**	0.917*	0.692	0.349	0.559	-0.292	1	-0.498	0.163	-0.317
<sup>226</sup> Ra	-0.442	-0.407	-0.219	-0.714	-0.984**	0.669	-0.494	-0.498	1	-0.129	0.960**
<sup>40</sup> K	0.787	0.318	-0.146	-0.145	0.114	-0.516	-0.402	0.163	-0.129	1	-0.177
<sup>232</sup> Th	-0.410	-0.246	-0.026	-0.491	-0.962**	0.912	-0.469	-0.317	0.960**	-0.177	1

Explanations:

\* The correlation is significant at the  $P < 0.05$  level (bilateral).

\*\* The correlation is significant at the  $P < 0.01$  level (bilateral).

Pearson correlation matrix between the different determined elements found in soil samples collected from Huancavelica, Peru.

#### 4. Conclusions

The concentrations of potential toxic elements and naturally occurring radioactive materials in soils from five districts in Huancavelica (Quintanilla Pampa (M1), San Cristóbal (M2), Yananaco (M3), Santa Ana (M4) and Asunción (M5)) have been assessed by XRF, ICP-MS and Gamma Spectroscopy. The results reveal that the past mining activities released high levels of As, Cd, Pb, Zn, Ni and Cu and perduring with time in all Huancavelica City. The highest levels of potential toxic elements are located in the Yananaco District which is closer to the abandoned mine than the other sites. However, the low levels of Hg in comparison to the local and international standards suggest that it has been moved although some amount remains maybe trapped in the soils, especially in the Yananaco District. The soil samples can be classified into two groups, depending on their radioactivities: M1, M3 and M5, with activity values above the world average, and group M2 and M4 showing average activities within the world range. The average dose rate (*D*) for the soil samples is 85.9 nGy/h, which is 1.7 times higher than the world average dose rate. Similarly, the average effective annual equivalent dose (*E*) is 0.105 mSv/y, which is 1.5 times higher than the world average. The overall results suggest that past mercury extraction in the mine enhanced the exposure of PTEs and NORM which remains spread around the City of Huancavelica today.

#### Acknowledgements

This work has been supported by a Collaboration Agreement between the University of Cambridge and the Universidad Nacional Autónoma de Huanta (Agreement G117323). JC Gonzalez thanks CONCYTEC – ProCiencia for funding the project entitled: “Fabrication and study of the direct current Josephson junction based on the macroscopic quantum effect of superconducting materials” through contract PE501082814-2023-PROCIENCIA. The authors are indebted to Mr. Raul Lopez Ccaico for his help during collection of samples.

#### Conflict of interest

The authors declare no conflict of interest. The authors declare that they have no known competing financial interests or personal relationships that could have appeared to influence the work reported in this paper. This research did not involve human or animal subjects.

#### Author Contributions

**Miguel Angel Castillo Corzo** – Conceptualization, Data curation, Funding acquisition, Investigation, Methodology, Validation, Writing – original draft. **Victor Antonio Peña Rodríguez** – Conceptualization, Data curation, Investigation, Methodology, Supervision, Validation, Visualization, Writing – review & editing. **Manuel A. Manrique Nugent** – Conceptualization, Methodology, Visualization, Writing – review & editing. **Eduardo G. Villarreyes Peña** – Conceptualization, Data curation, Investigation, Methodology, Validation, Writing – original draft. **Patrick**

**Byrne** – Conceptualization, Data curation, Investigation, Validation, Writing – review & editing. **Juan Carlos Gonzalez** – Conceptualization, Funding acquisition, Methodology, Validation, Visualization, Writing – review & editing. **Galo Patiño Camargo** – Conceptualization, Methodology, Visualization, Writing – review & editing. **Crispin H.W. Barnes** – Conceptualization, Data curation, Methodology, Supervision, Validation, Visualization, Writing – review & editing. **Jesus F. Sánchez Ortiz** – Conceptualization, Methodology, Visualization, Writing – review & editing. **Jose Saldaña Tovar** – Conceptualization, Methodology, Visualization, Writing – review & editing. **Luis De Los Santos Valladares** – Conceptualization, Data curation, Funding acquisition, Investigation, Methodology, Supervision, Validation, Visualization, Writing – original draft. All authors read and approved the final manuscript.

#### References

- Adukpo, O., Ahiamadjie, H., Tandoh, J., Gyampo, O., Nyarku, M., Darko, E., Faanu, A., Dampare, S., 2010. Assessment of NORM at diamond cement factory and its effects in the environment. *Journal of Radioanalytical and Nuclear Chemistry* 287, 87–92. <https://doi.org/10.1007/s10967-010-0844-6>
- Agency, E., 2007. UK Soil and Herbage Pollutant Survey. Report N° 7: Environmental concentrations of heavy metals in UK soil and herbage. UK: Environment Agency, pp 132.
- Agency, International Atomic Energy, 2016. Reference Sheet for IAEA-RGK-1. Seibersdorf: International Atomic Energy Agency. <https://analytical-reference-materials.iaea.org/iaea-rgk-1>
- Al-Jundi, J., Al-Bataina, J., Abu-Rukah, B., Shehadeh, H.M., 2003. Natural radioactivity concentrations in soil samples along the Amman Aqaba Highway, Jordan. *Radiation Measurements* 36(1–6), 555–560. [https://doi.org/10.1016/S1350-4487\(03\)00202-6](https://doi.org/10.1016/S1350-4487(03)00202-6)
- Al-Saleh, F., Al-Harshan, G., 2008. Measurements of radiation level in petroleum products and wastes in Rivadh city Refinery. *Journal Environ Radioact* 99, 1026–1031. <https://doi.org/10.1016/j.jenvrad.2007.12.002>
- Atibu, E., Arpagaus, P., Mulaji, C., Mpiana, P., Poté, J., Loizeau, J.L., Carvalho, F., 2022. High Environmental Radioactivity in Artisanal and Small-Scale Gold Mining in Eastern Democratic Republic of the Congo. *Minerals* 12(10), 1278.
- Ayala, L., 2020. Recuperación y conservación de los recursos hídricos para el mejoramiento ganadero en cabecera de la sub cuenca del rio Ichu del departamento de Huancavelica. *Huancavelica: Gerencia Regional de Recursos Naturales y Gestión Ambiental, Gobierno Regional de Huancavelica* 1(1), 633. [https://sinia.minam.gob.pe/sites/default/files/siar-huancavelica/archivos/public/docs/hidrologia\\_riochu-completo\\_0.pdf](https://sinia.minam.gob.pe/sites/default/files/siar-huancavelica/archivos/public/docs/hidrologia_riochu-completo_0.pdf)
- Baeza, A., Alonso, A., Heras, M., 2003. Procedimiento para la conservación y preparación de muestras de suelo para la determinación de la radiactividad. Madrid-España.: Consejo de Seguridad Nuclear (CSN). Retrieved from <https://www.csn.es/documents/10182/27786/INT-04-07+Vigilancia+radiol%C3%B3gica+ambiental-Procedimiento+1.2>
- Bailey, E., Gray, J., Theodorakos, P., 2002. Mercury in vegetation and soils at abandoned mercury mines in southwestern Alaska, USA. *Geochemistry: Exploration, Environment, Analysis* 2(3), 275–285. <https://doi.org/10.1144/1467-787302-032>
- Bakr, S., Sayed, M., Salem, K., Morsi, E., Masoud, M., Ezzat, E., 2023. Lead (Pb) and cadmium (Cd) blood levels and potential hematological health risk among inhabitants of the claimed hazardous region around Qaroun Lake in Egypt. *BMC Public Health* 23(1071), 2–11. <https://doi.org/10.1186/s12889-023-16007-w>

- Bech, J., Poschenrieder, C., Llugany, M., Barceló, J., Tume, J., Tobias, F., Barranzuela, J., Vásquez, E., (1997). Arsenic and heavy metal contamination of soil and vegetation around a copper mine in Northern Peru. *Science of The Total Environment* 203(1) 83–91. [https://doi.org/10.1016/S0048-9697\(97\)00136-8](https://doi.org/10.1016/S0048-9697(97)00136-8)
- Benson, J., Cheng, Y., Eidson, A., Hahn, F., Henderson, R., Pickrell, J., 1995. Pulmonary toxicity of nickel subsulfide in F344/N rats exposed for 1–22 days. *Toxicology* 103(1), 9–22. [https://doi.org/10.1016/0300-483x\(95\)03098-z](https://doi.org/10.1016/0300-483x(95)03098-z)
- Beretka, J., Matthew, P., 1985. Natural radioactivity of Australian building materials, industrial wastes and by-products. *Health Physics* 48(1), 87–95. <https://doi.org/10.1097/00004032-198501000-00007>
- Bergdahl, I., Skerfving, S., 2022. Chapter 19 – Lead. *Handbook on the Toxicology of Metals (Fifth Edition) II*, 427–493. <https://doi.org/10.1016/B978-0-12-822946-0.00036-2>
- Biester, H., Müller, G., Schöler, H., 2002. Binding and mobility of mercury in soils contaminated by emissions from chlor-alkali plants. *Science of The Total Environment* 284(1–3), 191–203. [https://doi.org/10.1016/S0048-9697\(01\)00885-3](https://doi.org/10.1016/S0048-9697(01)00885-3)
- Bishop, K., et al. 2020. Recent advances in understanding and measurement of mercury in the environment: Terrestrial Hg cycling. *Science of The Total Environment* 721, 137647. <https://doi.org/10.1016/j.scitotenv.2020.137647>
- Bissen, M., Frimmel, F., 2003. Arsenic a Review. Part II: Oxidation of Arsenic and its Removal in Water Treatment. *Acta hydrochimica et hydrobiologica* 31, 97–107
- Cancès, B., Juillot, F., Morin, G., Laperche, V., Polya, D., Vaughan, D., Hazemann J., Proux, O., Brown, J., Calas, G., 2008. Changes in arsenic speciation through a contaminated soil profile: A XAS based study. *Science of The Total Environment* 397, 178–189. <https://doi.org/10.1016/j.scitotenv.2008.02.023>
- Castillo, M., Borja, L., De Los Santos, L., Gonzales, J., Medina, J., Trujillo, A., Peña, V., 2022. Magnetic, structural and Mossbauer Study of soils from an ancient mining area in Huancavelica-Perú. *Hyperfine Interactions* 243(3), 1–16. <https://doi.org/10.1007/s10751-021-01786-8>
- Castro-Bedriñana, J., Chirinos-Peinado, D., Ríos-Ríos, E., 2013. Niveles de plomo en gestantes y neonatos en la ciudad de la Oroya, Perú. *Revista Peruana de Medicina Experimental y Salud Publica* 30(3), 393–398. <http://www.scielo.org.pe/pdf/rins/v30n3/a04v30n3.pdf>
- Chashschin, V., Artunina, G., Norseth, T., 1994. Congenital defects, abortion and other health effects in nickel refinery workers. *Science The Total Environment* 148(2–3), 287–91. [https://doi.org/10.1016/0048-9697\(94\)90405-7](https://doi.org/10.1016/0048-9697(94)90405-7)
- Cheng, H., Li, M., Zhao, C., Li, K., Peng, M., Qin, A., Cheng, X., 2014. Overview of trace metals in the urban soil of 31 metropolises in China. *Journal of Geochemical Exploration* 139, 31–52. <https://doi.org/10.1016/j.gexplo.2013.08.012>
- Choudhury, T., Ferdous, J., Haque, M., Rahman, M., Quraishi, S., Rahman, M., 2022. Assessment of heavy metals and radionuclides un groundwater and associated human health risk appraisal in the vicinity of Rooppur nuclear plant, Bangladesh. *Journal of Contaminant Hydrology* 251, 104072. <https://doi.org/10.1016/j.jconhyd.2022.104072>
- De Los Santos Valladares, L., Ccamapaza, J.L., Valencia-Bedregal, R.A., Borja-Castro, L.E., Velazquez-García, J., Nimalika Perera, D.H., Barnes, C., 2022. Physical and chemical characterization of sediments from an Andean river exposed to mining and agricultural activities: The Moquegua River, Peru. *International Journal of Sediment Research* 37, 780–793. <https://doi.org/10.1016/j.ijsrc.2022.06.002>
- De Los Santos Valladares, L., Vargas Luque, A., Borja Castro, L., Valencia Bedregal, R., Velazquez-García, J., Peregrine Barnes, E., William Barnes, C., 2024. Physical and chemical techniques for a comprehensive characterization of river sediment: A case of study, the Moquegua River, Peru. *International Journal of Sediment Research* 39, 478–494. <https://doi.org/10.1016/j.ijsrc.2024.03.003>
- Dev Singh, A., Khanna, K., Kour, J., Dhiman, S., Bhardwaj, T., Devi, K., Bhardwaj, R., 2023. Critical review on biogeochemical dynamics of mercury (Hg) and its abatement strategies. *Chemosphere* 319, 137917. <https://doi.org/10.1016/j.chemosphere.2023.137917>
- Douglas, G., Reddy, S., Saxey, D., MacRae, C., Webster, N., Beeching, L., 2023. Engineered mineralogical interfaces as radionuclide repositories. *Scientific Reports* 13, 2121. <https://doi.org/10.1038/s41598-023-29171-1>
- El-Taher, A., Makhluaf, S., 2010. Natural radioactivity levels in phosphate fertilizer and its environmental implications in Assuit governorate, Upper Egypt. *Indian journal of Pure and Applied Physics* 48(10), 697–702. <https://nopr.niscares.in/bitstream/123456789/10389/1/IJ-PAP%2048%2810%29%20697-702.pdf>
- Fernandez, B., Mullisaca, E., Huanchi, L., 2022. Level of soil contamination with arsenic and heavy metals in Tiquillaca (Peru). *Journal of High Andean Research* 24(2), 131–138. <http://dx.doi.org/10.18271/ria.2022.416>
- Florida, N., 2021. Cadmium in soil and cacao beans of Peruvian and South American origin. *Revista Facultad Nacional de Agronomía Medellín* 74(2), 9499–9515. <https://doi.org/10.15446/rfnam.v74n2.91107>
- Foulds, S., Brewer, P., Macklin, M., Haresign, W., Betson, R., Rassner, S., 2014. Flood-related contamination in catchments affected by historical metal mining: An unexpected and emerging hazard of climate change. *Science of The Total Environment* 476–477(1), 165–180. <https://doi.org/10.1016/j.scitotenv.2013.12.079>
- Gaioli, M., Amoedo, D., González, D., 2012. Impacto del mercurio sobre la salud humana y el ambiente. *Arch Argent Pediatr* 110(3), 259–264. <http://www.dx.doi.org/10.5546/aap.2012.259>
- Galhardi, J., García-Tenorio, R., Bonotto, D., Díaz, I., Motta, J., 2017. Natural radionuclides in plants, soils and sediments affected by U-rich coal mining activities in Brazil. *Journal of Environmental Radioactivity* 177, 37–47. <https://doi.org/10.1016/j.jenvrad.2017.06.001>
- Gazineu, M., Hazin, C., 2008. Radium and potassium-40 in solid wastes from the oil industry. *Applied Radiation and Isotopes* 66(1), 90–94. <https://doi.org/10.1016/j.apradiso.2007.07.012>
- Gilli, R., Karlen, C., Weber, M., Rüegg, J., Barmettler, K., Biester, H., Kretzschmar, R., 2018. Speciation and Mobility of Mercury in Soils Contaminated by Legacy Emissions from a Chemical Factory in the Rhône Valley in Canton of Valais, Switzerland. *Soil Systems* 2(44), 22. <https://doi.org/10.3390/soilsystems2030044>
- Gnamuš, A., Byrne, A., Horvat, M., 2000. Mercury in the Soil-Plant-Deer-Predator Food Chain of a Temperate Forest in Slovenia. *Environmental Science & Technology* 34(16), 3337–3345. <http://dx.doi.org/10.1021/es991419w>
- Gosar, M., Šajn, R., Biester, H., 2006. Binding of mercury in soils and attic dust in the Idrija mercury mine area (Slovenia). *Science of The Total Environment* 369(1–3), 150–162. <https://doi.org/10.1016/j.scitotenv.2006.05.006>
- Gussone, N., Böhm, F., Eisenhauer, A., Dietzel, M., Heuser, A., Teichert, B., Wolf, C., 2005. Calcium isotope fractionation in calcite and aragonite. *Geochimica et Cosmochimica Acta* 69(18), 4485–4494. <https://doi.org/10.1016/j.gca.2005.06.003>
- Hagan, N., 2014. Residential Mercury contamination and Exposure in Huancavelica, Perú. University of North Carolina at Chapel Hill. <https://doi.org/10.17615/vdda-sc67>
- Hagan, N., Robins, N., Espinoza, R., Hsu-Kim, H., 2015. Speciation and bioaccessibility of mercury in adobe bricks and dirt floors in Huancavelica. *Environmental Geochemistry and Health*, 37, 263–272. <https://doi.org/10.1007/s10653-014-9644-1>
- Halbach, K., Mikkelsen, Ø., Berg, T., Steinnes, E., 2017. The presence of mercury and other trace metals in surface soils in the Norwegian Arctic. *Chemosphere* 188, 567–574. <https://doi.org/10.1016/j.chemosphere.2017.09.012>
- Hamlat, M., Djeflal, S., Kadi, H., 2001. Assessment of radiation exposures from naturally occurring radioactive materials in the oil and gas

- industry. *Applied Radiation and Isotopes* 55(1), 141–146. [https://doi.org/10.1016/S0969-8043\(01\)00042-2](https://doi.org/10.1016/S0969-8043(01)00042-2)
- Handbook of Radiatioactivity Analysis Vol 1: Radiation Physic an Detectors. Academic Press, Elsevier 2020 ISBN 978-0-12-814397-1, <https://doi.org/10.1016/C2016-0-04811-8>
- He, S., He, Z., Yang, X., Stoffella, P., Baligar, V., 2015. Chapter Four-Soil Biogeochemistry, Plant Physiology, and Phytoremediation of Cadmium-Contaminated Soils. *Advances in Agronomy* 134, 135–225. <https://doi.org/10.1016/bs.agron.2015.06.005>
- Higueras, P., Oyarzun, R., Biester, H., Lillo, H., Lorenzo, J., 2003. A first insight into mercury distribution and speciation in soils from the Almadén mining district, Spain. *Journal of Geochemical Exploration* 180(1), 95–104.
- Huerta Alata, M., Alvarez-Risco, A., Suni Torres, L., Moran, K., Pilares, D., Carling, G., Yáñez, J., 2023. Evaluation of Environmental Contamination by Toxic Elements in Agricultural Soils and Their Health Risks in the City of Arequipa, Peru. *Sustainability* 15(4), 3829. <https://doi.org/10.3390/su15043829>
- Hunter, M., Perera, D., Barnes, E., Lepage, H., Escobedo Pacheco, E., Idros, N., Barnes, C., 2024. Landscape-Scale Mining and Water Management in a Hyper-Arid Catchment: The Cuajone Mine, Moquegua, Southern Peru. *Water* 16(769), 28. <https://doi.org/10.3390/w16050769>
- International Atomic Energy Agency (IAEA), 2011. Referencia Material. Viena: International Atomic Energy Agency. <https://analytical-reference-materials.iaea.org/catalogs>
- International Atomic Energy Agency (IAEA), 2012. Extent of Environmental by Naturally Occurring Radioactive Material (NORM) and Technological Options for Mitigation. Technical Reports Series N° 419. New York: IAEA.
- International Organization for Standardization (ISO), 2015. ISO: 18589–3. Medición de la radiactividad en el medio ambiente. Suelo. Parte3. <https://www.iso.org/standard/82294.html>
- International Atomic Energy Agency (IAEA), 2016. Reference Sheet for IAEA-RGTh-1 thorium. Seibersdorf: International Atomic Energy Agency. <https://analytical-reference-materials.iaea.org/iaea-rgth-1>
- International Atomic Energy Agency (IAEA), 2019. Certified Reference IAEA-412. Viena: International Atomic Energy Agency. <https://analytical-reference-materials.iaea.org/iaea-412>
- International Atomic Energy Agency (IAEA), 2019. Determination and interpretation. International Atomic Energy Agency.
- International Atomic Energy Agency (IAEA), 2021. Referencia Certificad IAEA-447. Seibersdorf: International Atomic Energy Agency. <https://analytical-reference-materials.iaea.org/iaea-447>
- International Organization for Standardization (ISO), 2019. ISO: 19581. Medición de la Radiactividad-Radionucleidos emisores de rayos gamma-Método de cribado rápido mediante espectrometría de rayos gamma con detectores de centello. <https://www.iso.org/standard/65307.html>
- Kabata-Pendias, A., Pendias, H., 2001. Trace Elements in Soil and Plants (3<sup>rd</sup> ed.). (CRC, Ed.) Florida, EE.UU.: CRC-Press, Boca Raton London New York Washington, D.C. Pp. 403.
- Kaniu, M., Angeyo, H., Darby, I., Muia, L., 2018. Rapid in-situ radiometric assessment of the Mrima-Kiruku high background radiation anomaly complex of Kenya. *Journal of Environmental Radioactivity* 188, 47–57. <https://doi.org/10.1016/j.jenvrad.2017.10.014>
- Karahan, G., Bayulken, A., 2000. Assessment of gamma dose rates around Istanbul (Turkey). *Journal of Environmental Radioactivity* 47(2), 213–221. [https://doi.org/10.1016/S0265-931X\(99\)00034-X](https://doi.org/10.1016/S0265-931X(99)00034-X)
- Kim, K., Churchill, D., 2011. Phosphorus: Radionuclides. *Encyclopedia of Inorganic and Bioinorganic Chemistry*. <https://doi.org/10.1002/9781119951438.eibc0418>
- Krishna, A., Govil, P., 2007. Soil Contamination Due to Heavy Metals from an Industrial Area of Surat, Gujarat, Western India. *Environmental Monitoring and Assessment* 124, 263–275 (2007). <https://doi.org/10.1007/s10661-006-9224-7>
- Kubier, A., Wilkin, R., Pichler, T., 2019. Cadmium in soils and groundwater: A review. *Applied Geochemistry* 108, 104388. <https://doi.org/10.1016/j.apgeochem.2019.104388>
- Li, S., Jia, Z., 2018. Heavy metals in soils from a representative rapidly developing megacity (SW China): Levels, source identification and apportionment. *Catena* 163, 414–423. <https://dx.doi.org/10.1016/j.catena.2017.12.035>
- Liu, Y., Zhou, W., Gao, B., Zheng, Z., Chen, G., Wie, Q., He, Y., 2021. Determination of radionuclide concentration and radiological hazard in soil and water near the uranium tailing reservoir in China. *Environmental Pollutants and Bioavailability* 33(1), 174–183. <https://doi.org/10.1080/26395940.2021.1951123>
- Manta, D., Angelone, M., Bellanca, A., Neri, R., Sprovieri, M., 2002. Heavy metals in urban soils: a case study from the city of Palermo (Sicily), Italy. *Science of The Total Environment* 300(2), 229–243. [https://doi.org/10.1016/S0048-9697\(02\)00273-5](https://doi.org/10.1016/S0048-9697(02)00273-5)
- Matisoff, G., Whiting, P., 2011. Measuring Soil Erosion Rates Using Natural (<sup>7</sup>Be, <sup>210</sup>Pb) and Anthropogenic (<sup>137</sup>Cs, <sup>239,240</sup>Pu) Radionuclides. *Handbook of Environmental Isotope Geochemistry I*, 487–519. [https://doi.org/10.1007/978-3-642-10637-8\\_25](https://doi.org/10.1007/978-3-642-10637-8_25)
- Ministerio de Agricultura y Riego del Perú (MIDAGRI), 2009. Huancavelica: Ministerio Agricultura, pp 20. <https://www.midagri.gob.pe/portal/download/pdf/especiales/aliados/Huancavelica.pdf>
- Ministerio del Ambiente, 2017 (MINAM). Estándares de Calidad Ambiental – Decreto Supremo N° 011–2017-MINAM. Ministerio del Ambiente – MINAM. Lima: Diario El Peruano, pp 4. [https://www.minam.gob.pe/wp-content/uploads/2017/12/DS\\_011-2017-MINAM.pdf](https://www.minam.gob.pe/wp-content/uploads/2017/12/DS_011-2017-MINAM.pdf)
- Ministerio de Transporte de Comunicaciones (MTC), 2022. El Anuario Estadístico 2022. Lima: Oficina Estadística del Ministerio de Transporte y Comunicaciones, pp 237. <https://cdn.www.gob.pe/uploads/document/file/4577337/Anuario%20Estad%20C3%ADstico%202022.pdf>
- Mohuba, S., Abiye, T., Nhleko, S., 2022. Evaluation of Radionuclide Levels in Drinking Water from Communities near Active and Abandoned Gold Mines and Tailings in the West Rand Region, Gauteng, South Africa. *Minerals* 12(11), 1370. <https://doi.org/10.3390/min12111370>
- Moshupya, M., Mohuba, S., Abiye, T., Korir, I., Nhleko, S., Mkhosi, M., 2022. In Situ Determination of Radioactivity Levels and Radiological Doses in and around the Gold Mine Tailing Dams, Gauteng Province, South Africa. *Minerals* 12(10), 1295. <https://doi.org/10.3390/min12101295>
- Orellana, E., Pérez, L., Custodio, M., Bulege, W., Yallico, L., Cuadrado, W., 2021. Cadmium, Lead and Zinc in the Soil-Plant-Alpaca System and Potential Health Risk Assessment Associated with the Intake of Alpaca Meat in Huancavelica, Peru. *Journal of Ecological Engineering* 22(3), 40–52. <https://doi.org/10.12911/22998993/132175>
- Osterwalder, S., et al, 2019. Mercury emission from industrially contaminated soils in relation to chemical, microbial, and meteorological factors. *Environmental Pollution* 250, 944–952. <https://doi.org/10.1016/j.envpol.2019.03.093>
- Paktun, D., Foster, A., Heald, S., Laflamme, G., 2004. Speciation and characterization of arsenic in gold ores and cyanidation tailings using X-ray absorption spectroscopy. *Geochimica et Cosmochimica Acta* 68(5), 969–983. <https://doi.org/10.1016/j.gca.2003.07.013>
- Parmaksiz, A., Ozkov, Y., Agus, Y., 2023. Natural radioactivity of a copper-zinc mine with a production facility in Turkiye and radiological consequences of usage of the tailing as a concrete additive. *Journal of Radioanalytical and Nuclear Chemistry* 332, 211–223. <https://doi.org/10.1007/s10967-022-08751-x>
- Perevoshchikov, R., Perminova, A., Menshikova, E., 2022. Natural radionuclides in soils of natural-technogenic landscapes in the impact zone of potassium salt mining. *Minerals* 12(11), 1352. <https://doi.org/10.3390/min12111352>
- Ponce, J., Van Geen, A., Landes, F., Palacios, E., Ponce, P., Languasco, J., Vargas, R., 2024. Assessing Risk Levels of Lead Presence in Residential Soils: A Case Study in Lima, Peru. *Journal, ISEE Conference Abstracts* (1). <https://doi.org/10.1289/isee.2024.0877> Puga, S., Sosa, M.,

- Lebgue, T., Quintana, C., Campos, A., 2006. Contaminación por metales pesados en suelos provocados por la industria minera. *Ecología Aplicada* 5(1,2), 149–155.
- Quintana, B., Pérez Iglesias, J., 2004. Selección, preparación y uso de patrones para espectroscopia gamma. Madrid: Consejo de Seguridad Nuclear. <https://www.csn.es/documents/10182/27786/INT-04-07+Vigilancia+radio%3%B3gica+ambiental.+Procedimiento+1.4/35754ad8-0a52-4a62-83f1-07d70b7d83f9>
- Rahim, H., Akbar, W., Alatalo, J., 2022. A Comprehensive Literature Review on Cadmium (Cd) Status in the Soil Environment and Its Immobilization by Biochar-Based Materials. *Agronomy* 12(4), 877. <https://doi.org/10.3390/agronomy12040877>
- Ramirez, A., 1986. Cadmium pollution in La Oroya, Peru. *La Oroya, Perú: Bulletin of the Pan American Health Organization (PAHO)* 20(4). <https://iris.paho.org/handle/10665.2/27219>
- Ramirez, A., 2008. Intoxicación ocupacional por mercurio. *Anales de la Facultad de Medicina* 69(1), 46–51. <http://www.scielo.org.pe/pdf/afm/v69n1/a10v69n1.pdf>
- Rani, A., Singh, S., 2005. Natural radioactivity levels in soil samples from some areas of Himachal Pradesh, India using  $\gamma$ -ray spectrometry. *Atmospheric Environment* 39(34), 6306–6314. <https://doi.org/10.1016/j.atmosenv.2005.07.050>
- Robins, N., 2011. Mercury, mining and empire, The human and ecological costs of colonial silver mining in the Andes. *Indiana University Press*, pp 320.
- Rodrigues, S., et al, 2006. Mercury in urban soils: A comparison of local spatial variability in six European cities. *Science of The Total Environment* 368(2–3), 926–936. <https://doi.org/10.1016/j.scitotenv.2006.04.008>
- Rollog, M., Cook, N., Guagliardo, P., Ehrig, K., Kilburn, M., 2020. Radionuclide distributions in Olympic Dam copper concentrates: The significance of minor hosts, incorporation mechanisms, and the role of mineral surfaces. *Minerals Engineering* 148, 106176. <https://doi.org/10.1016/j.mineng.2019.106176>
- Salas-Mercado, D., Hermoza-Gutierrez, M., Belizario-Quispe, G., Chaiña, F., Quispe, E., Salas-Ávila, D., 2022. Geochemical Indices for the Assessment of Chemical Contamination Elements in Sediments of the Suches River, Peru. *Pollution* 8(2), 595–610, doi: 810.22059/POLL.2021.331806.1205
- Satoshi, U., Stephen, P., Blum, J., Rodney, E., 2003. Nanoscale mineralogy of arsenic in a region of New Hampshire with elevated As-concentrations in the groundwater. *American Mineralogist* 88, 1844–1852. <https://doi.org/10.2138/am-2003-11-1227>
- Sharma, R., Ramteke, S., Patel, K., Kumar, S., Sarangi, B., Agrawal, S., Lata, L., Milosh, H., 2015. Contamination of Lead and Mercury in Coal Basin of India. *Journal of Environmental Protection* 6(12), 1430–1441. <http://dx.doi.org/10.4236/jep.2015.612124>
- Schnitzer, M., Turner, R., Hoffman, I., 1964. A Thermogravimetric study of organic matter of representative canadian podzol soils. *Canadian Journal of Soil Science* 44(1), 7–13.
- Servicio Nacional de Sanidad Agraria (SENASA), 2012. Enero 31. Resolución Jefatural N° 0013–2012-AG-SENASA. *El Peruano*, pp. 460175–460177.
- Smialowicz, R., Rogers, R., Riddle, M., Stott, G., 1984. Immunologic effects of nickel: I. Suppression of cellular and humoral immunity. *Environmental Research* 33(2), 413–27. [https://doi.org/10.1016/0013-9351\(84\)90039-2](https://doi.org/10.1016/0013-9351(84)90039-2)
- Soares, L., Egreja, F., Linhares, L., Windmoller, C., Yoshida, M., 2015. Acumulación y oxidación de mercurio elemental en suelos tropicales. *Chemosphere* 134, 181–191. <https://doi.org/10.1016/j.chemosphere.2015.04.020>
- Steinnes, E., Berg, T., Sjøbakk, T., 2003. Temporal and spatial trends in Hg deposition monitored by moss analysis. *Science of The Total Environment* 304(1–3), 215–219. [https://doi.org/10.1016/S0048-9697\(02\)00570-3](https://doi.org/10.1016/S0048-9697(02)00570-3)
- Tapia, J., Murray, J., Ormachea, M., Tirado, N., Nordstrom, D., 2019. Origin, distribution, and geochemistry of arsenic in the Altiplano-Puna plateau of Argentina, Bolivia, Chile, and Perú. *Science of The Total Environment* 678 (15) 309–325. ISSN 0048–9697. <https://doi.org/10.1016/j.scitotenv.2019.04.084>
- Taylor, M., 2015. Soil quality monitoring in the Waikato Region 2013. *New Zealand: Waikato Regional Council Technical Report 2013/49*, pp 45. <https://www.waikatoregion.govt.nz/assets/WRC/WRC-2019/TR201541.pdf>
- The Center for disease Control and Prevention CDC., 2022. The Adult Blood Lead Epidemiology and Surveillance (ABLES). <https://www.cdc.gov/niosh/lead/about/index.html>
- The National Institute for Occupational Safety and Health (NIOSH), 2022. The Center for Disease Control and Prevention (CDC).
- Tijhuis, L., Brattli, B., Sæther, O., 2002. A Geochemical Survey of Topsoil in the City of Oslo, Norway. *Environmental Geochemistry and Health* 24, 67–94. <https://doi.org/10.1023/A:1013979700212>
- Tóth, G., Hermann, T., Szatmári, G., Pásztor, L., 2016. Maps of heavy metals in the soils of the European Union and proposed priority areas for detailed assessment. *Science of The Total Environment* 565, 1054–1062. <https://doi.org/10.1016/j.scitotenv.2016.05.115>
- Torres, F., De la Torre, G., 2022. Mercury pollution in Peru: geographic distribution, health hazards, and sustainable removal technologies. *Environmental Science Polluty Research* 29(36), 54045–54059. <https://doi.org/10.1007/s11356-022-21152-7>
- Tsolova, V., Lazarova, R., Yordanova, I., Staneva, D., 2022. Radioactivity of soils enriched with pyrogenic artefacts in the land of Pernik city, Bulgaria. *Soil Science Annual* 73(2), 150764. <https://doi.org/10.37501/soilsa/150764>
- United Nations Scientific Committee on the Effects of Atomic Radiation (UNSCEAR), 2008. *Source And Effects Of Ionizing Radiation*. United Nations Publication. [https://www.unscear.org/unscear/uploads/documents/unscear-reports/UNSCEAR\\_2008\\_Report\\_Vol.I-CORR.pdf](https://www.unscear.org/unscear/uploads/documents/unscear-reports/UNSCEAR_2008_Report_Vol.I-CORR.pdf)
- Uzarowicz, Ł., Stobiński, M., Jędrzejek, F., Szarłowicz, K., Murach, D., 2024. Radioactivity of Technosols on thermal power station ash disposal sites: Assessment of potential radiological human-health risk. *Land Degradation & Development* 35(13), 4093–4104. <https://doi.org/10.1002/ldr.5207>
- Van Geen, A., Bravo, C., Gil, V., Sherpa, S., Jack, D., 2012. Lead exposure from soil in Peruvian mining towns: a national assessment supported by two contrasting examples. *Bulletin of the World Health Organization* 90(12), 878–886.
- Vasconcelos, D., Pereira, C., Oliveira, A., Santos, T., Reis, P., Rocha, Z., 2011. Natural radioactivity in sand beaches of Guarapari, Espírito Santo state, Brazil: a comparative study. *Belo Horizonte, Brazil*, pp 7.
- Waldron, H.A., 1980. *Metals in the Environment*. London, New York: Academic Press, 1980. Print, pp 333.
- Wang, J., Feng, X., Anderson, C., Xing, Y., Shang, L., 2012. Remediation of mercury contaminated sites – A review. *Journal of Hazardous Materials* 221–222, 1–18. <https://doi.org/10.1016/j.jhazmat.2012.04.035>
- Williams, M., Fordyce, F., Pajitprapapon, A., Charoenchaisri, P., 1996. Arsenic contamination in surface drainage and groundwater in part of the southeast Asian tin belt, Nakhon Si Thammarat Province, Southern Thailand. *Environmental Geology* 27, 16–33. <https://doi.org/10.1007/BF00770599>
- Xinwei, L., Xiaolan, Z., 2006. Measurement of natural radioactivity in sand samples collected from the Baoji Weihe Sands Park, China. *Environmental Geology* 50, 977–982. <https://doi.org/10.1007/s00254-006-0266-5>